



Evaluation OF Petrophysical And Hydrocarbon Potentiality For The Nubia A, Ras Budran Oil Field, Gulf Of Suez, Egypt.

Ahmed Galal¹, Mohamed Kassab², Waleed Osman³



CrossMark

1. Geology Dept., Faculty of Pet. & Min. Eng., Suez University, Suez, Egypt.

2. Dept., of Exploration, Egyptian Petroleum Research Institute (EPRI), Cairo, Egypt.

3. Geology Dept., Faculty of Pet. & Min. Eng., Suez University, Suez, Egypt. and Petroleum Eng. & Gas Technology Dept., The British University in Egypt, (B.U.E).

Abstract

The present study deals with the Petrophysical Evaluation of **Nubia A** of Lower Cretaceous age in Nubia Formation, Ras Budran oil field, Gulf of Suez, Egypt. The petrophysical parameters results of **Nubia A** in Nubia Formation is represented laterally (Iso-parametric maps, such as effective porosity, shale content, net-pay thickness and hydrocarbon saturation maps). A set of well logs has been run for the selected four wells. These wells named (RB-A1, RB-B1, RB-B11 and RB-C1). The minimum suite of logs consisted of gamma ray, density, neutron, and resistivity logs, all the log data are in the form of LAS files.

Nubia Formation is very good reservoir rock in most intervals, where the interpretation of the well logging data indicates that the total porosity ranges from 13.8% to 15%, effective porosity ranges from 13.2% to 15%, shale content ranges between 0.3% to about 2.1%, water saturation from 15.4% to about 52.1%, hydrocarbon saturation ranges from 47.9% to 84.6% and Netpay thickness ranges between 21 ft to about 137.25 ft. From Lithological Identification Techniques for Nubia A indicates the presence of mixed lithology has sandstone, shale, dolomite and limestone. The developments in Ras Budran field for **Nubia A** towards the central part around RB-B1 well and northwest- southeast, this shown by the increasing of effective porosity and hydrocarbon saturation respectively. There is a good opportunity to drill other Exploratory and development wells to enhance the productivity of the study area because it is containing valuable amount of hydrocarbon accumulation. The best well for this study is RB-A1 has high hydrocarbon saturation 76.2%, effective porosity 13.7% and Net pay thickness 137.25 ft.

Key Words

Petrophysics; Hydrocarbon; Porosity; Nubia Formation; Ras Budran oil field; Gulf of Suez

1. Introduction

The Gulf of Suez region is the narrow body of water, orientated in a North/North West-South/South East direction, separating the North-East corner of the African continent from the Sinai Peninsula. The Gulf of Suez area lies within the northern arm of the Red Sea rift. This area is the most actively explored area in Egypt and represents the most density drilled and explored part. It contains more than 80 oil fields in reservoirs that vary from the Precambrian to Quaternary in age (Schlumberger, 1995; El Nady et al., 2015).

The Gulf of Suez Basin is subdivided into three structural provinces based on the regional dip direction of its tilted fault blocks; the northern and southern provinces dip to the SW, whereas the

central province has a NE dip direction. These provinces are separated by two NE-trending accommodation zones (Moustafa, 1976; Patton et al., 1994; El Sawy., 2016).

Hence, Gulf of Suez is considered as a rift basin measuring 320 km in length by 60 - 25 km in width. It is an area of complex tectonics with faulted blocks limited by major NW-SE faults (Clysmic direction) and by subordinated SW-NE trending faults. And it is considered the most producer oil rift basin in the Middle East and Africa. (Schlumberger, 1995; El Nady et al., 2015).

Ras Budran oil field is one of the Gulf of Suez fields which are located in the central province of the eastern coast of the Gulf of Suez where the dip regime of the pre-Miocene is to the North-East. It is in the North of Belayim offshore concession area,

*Corresponding author e-mail: mkassab68@yahoo.com; welyosman@hotmail.com; ahmedgalal389@yahoo.com.

Receive Date: 07 February 2021, Revise Date: 10 March 2021, Accept Date: 17 March 2021

DOI: 10.21608/EJCHEM.2021.62045.3334

©2021 National Information and Documentation Center (NIDOC)

(Figure 1) approximately 4 km west to Sinai coast of Gulf of Suez and 13 km North-West of Abu Rudeis, bounded by latitudes $28^{\circ} 58'57''$ – $28^{\circ} 57'36''$ N and longitudes $33^{\circ} 08' 29''$ - $33^{\circ} 07' E$.

A sedimentary sequence ranging in age from Precambrian to Recent with non-depositional and erosional hiatuses are present in Ras Budran. The stratigraphic sequence is similar to the normal Gulf of Suez one (Figure 2).

The stratigraphic units in the Gulf of Suez region range in age from Precambrian to Recent. The geological section consists mainly of three phases; the first phase is represented by the age from Devonian to Eocene comprises the deposition of formations. These formations are important reservoir rocks, which include the Nubia sands. The second phase is characterized by source, reservoir and seal rocks and is represented by the Early Miocene. The third phase, of Late-Middle Miocene to Late Miocene and Pliocene age which acting as the essential cap rock and/or seal of the oil accumulation with no importance as source, or reservoir (Ghorab, 1961; Abd El Gawad, 1970; Zein El-Din et al, 1997; Azab et al., 2019). The pre-rift stratigraphic sequence is composed of strata ranging from Precambrian to Upper Eocene and contains sand, shale, and carbonate facies that were laid down under marine platform and terrestrial Environments. This period of sedimentation was affected by the failure to sequence the sedimentation of layers or erosion at different geologic times represented by major unconformities, (Alsharhan, 2003). The basement of the sedimentary sequence of The Suez graben was formed by sills of basic intrusive, dyke sand a great variety of crystalline. Different types of rocks are recognized such as crystalline schists, granites, porphyrites and gneisses (Schlumberger, 1984). Basement samples are composed of potassium feldspars, quartz, with patches of light green minerals and dark grey mica (biotite) (Zahran and Meshref, 1988). Granite outcrops are abundant and their erosional products were the main source of coarse clastics which form the predominant reservoirs of the Suez graben, ranging in age from Paleozoic to Mesozoic and Tertiary (Schlumberger, 1984).

Basement rocks are overlain by a wedge of coarse clastic deposits, characterized by poorly sorted, pebbly, coarse grained sandstone. A Devonian age is assigned to this series because of its position below dated marine Lower Carboniferous. These sandstones, referred to as the Nubia D sandstones, reach a maximum thickness of about 1312ft. They make up one of the main pay zones in the Hurgada, Ramadan, Ras Gharib, and July fields

(Schlumberger, 1984).

The term Nubia was introduced to describe a massive clastic section which covers the northern Sudan and southern part of Egypt (Russeger, 1937). Gradually the term was used to include all the sand bodies below the Late Cretaceous carbonates to Cambrian (Said, 1962; Beleity et al., 1986). Nubia "A" and Nubia "B" are composed of sandstone and essentially dark colored shale respectively. The Nubia sandstone section is an excellent reservoir rock for oil accumulation. In fact; it is one of the main pay zones in, Ras Gharib, July, Ras Budran oilfields and secondary pay at Bakr oilfield (Bobbitt and Gallagher, 1978). Nubia "B" facies is mainly composed of dark grey and black dense shale with some interlayers of light grey and brownish grey sand. Regionally, to the north, Nubia "B" rests on Nubia "C" unit with probable disconformity (Steen, 1982). The Devonian sandstone is overlain by the Early Carboniferous marine black shales of the Nubia B. They appear to be a poor source rock due to their low content of organic matter and because they are highly hardened. They may, however, function as sufficient seals. Maximum thickness of the Carboniferous black shales is about 200m. The Nubia B Formation has been encountered in the Ras Gharib, Bakr, Kareem Morgan, and more recent fields (Schlumberger, 1984).

2. Methods and Techniques

The main task of well log analysis is petrophysical evaluation. This destination is to estimate the volume of shale, water saturation, porosity, net Pay and hydrocarbon saturation at a reservoir. The procedures of well log analysis which performed in this study are consisting of two phases; Data gathering, Database editing task and petrophysical evaluation tasks

Different wire line logging suites (Gamma ray, Neutron, Density, Resistivity, etc.) for Four wells, namely, RB-A1, RB-B1, RB-B11 and RB-C1 are used in the analysis and performing the necessary calculations. The shale volume, effective porosity and fluid saturation (hydrocarbon and water) are the most important and necessary petrophysical parameters for characterizing the potential reservoirs.

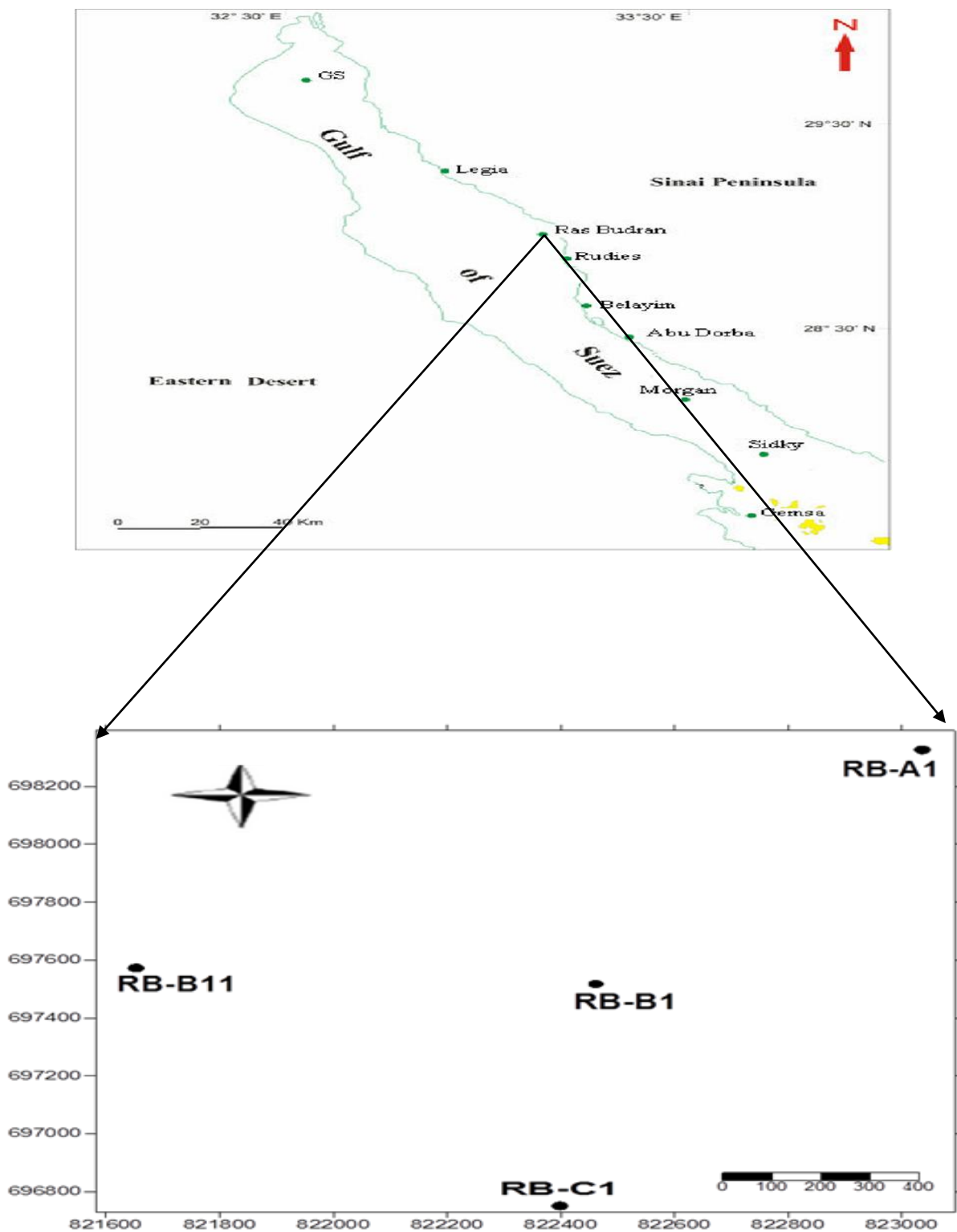


Figure 1 Location map of the study area showing the available wells

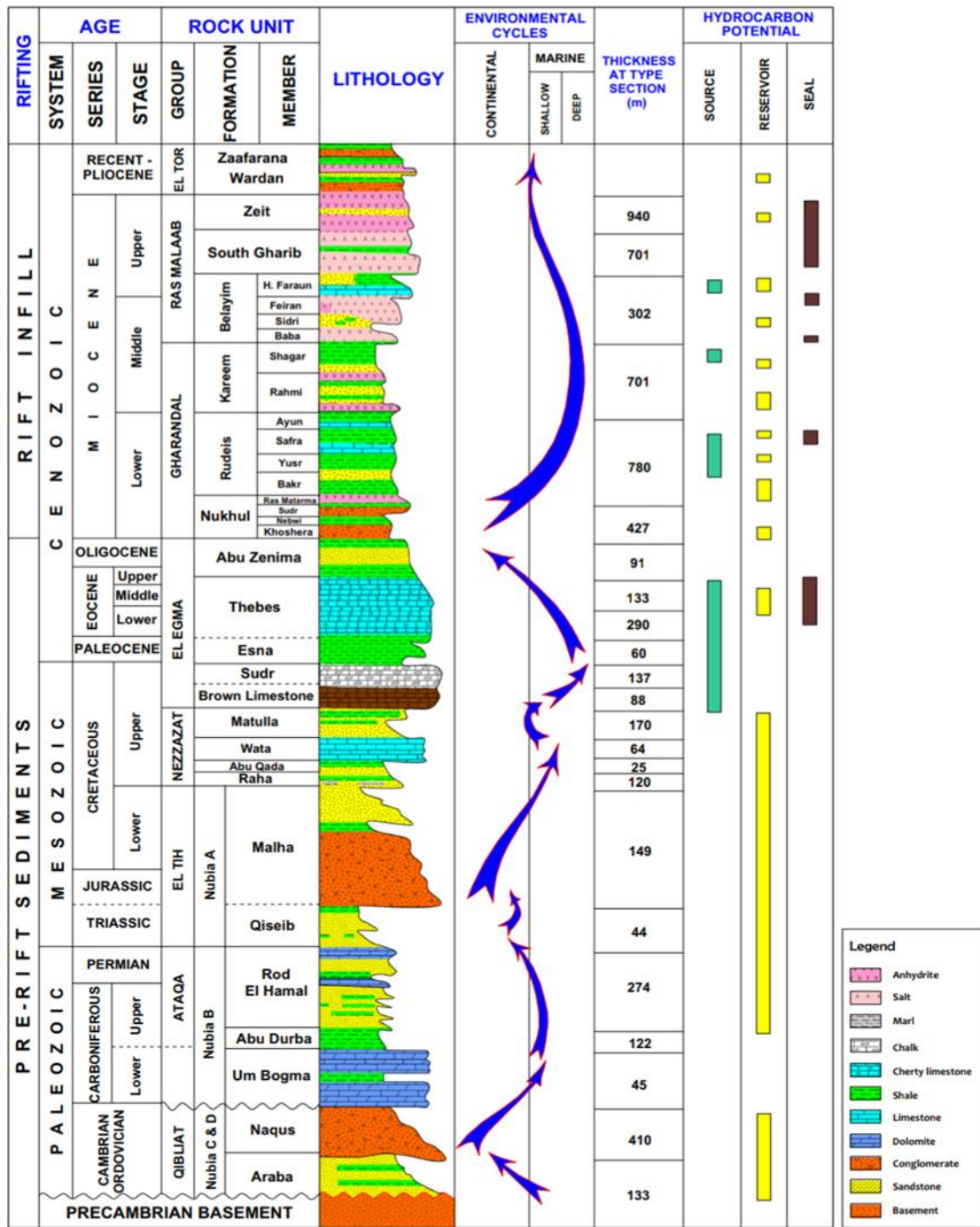


Figure 2 Summary stratigraphy of the central Gulf of Suez (modified after Alsharhan and Salah 1995)

In the present study, the open-hole log data for the studied wells are in the form of LAS files; these data were collected and digitized. The available open-hole well logging tools for the four wells that are used in the present study are:

Well Name	Available Logs
RB-A	GR Caliper, MSFL, LLS, LLD, ΔT , RHOB, DEN, NC
RB-B1	GR, Caliper, MSFL, LLS, LLD, ΔT , RHOB, DEN, NC
RB-B11	GR, ILM, LLS, RHOB, ILD
RB-C1	GR, MSFL, LLS, LLD, NC, RHOB, ILD

Where; GR: Gamma ray curve, MSFL: Microphysical resistivity curve, LLS: Shallow resistivity curve, LLD: Deep resistivity curve, DEN: Density curve, NC: Neutron curve, ΔT : Interval Transit Time Curve, RHOB: Bulk Density curve, ILD: Induction Deep Resistivity, ILM: Induction Medium Resistivity

The analysis, which has been carried out for different well logs (Density, Neutron, Sonic, Gamma ray, Resistivity, etc.), was interpreted to evaluate the hydrocarbon potentiality of Nubia Formation. This analysis has been carried out using Techlog Schlumberger software 2015.3.

Well log analysis is the most important function for any well after drilling, to detect the reservoir rocks among the all drilled formations. Logging data is used to identify productive zones via define physical rock characteristics (such as lithology, porosity, water saturation and hydrocarbon saturation), to determine depth and thickness of Netpay zones, to classification between hydrocarbon and water in a reservoir, and to

Estimate hydrocarbon reserves. Geologic maps developed from log interpretation help drilling locations.

2.1 Determination of shale content (V_{sh})

2.1.1 Gamma-Ray Method: The gamma ray log is an extremely simple and useful log that is used in all petrophysical interpretations and considered to be one of the best tools used for determining and identifying the shale volume this is especially due to its sensitive response for the radioactive materials normally concentrated in the Shaly rocks. Equation no1

$$V_{SH}=0.083[2^{(s.7 \times IGR)} - 1.0]$$

Where

$$IGR = \frac{GR_{log} - GR_{sand}}{GR_{shale} - GR_{sand}} \quad (1)$$

2.1.2 Neutron –Density

$$V_{sh} = \frac{X1 - X0}{X2 - X0} \quad (2)$$

$$X0 = NPHI_{ma}, X1 = NPHI + M1 (RHOB_{ma} - RHOB),$$

$$X2 = NPHI_{sh} + M1 (RHOB_{ma} - RHOB_{sh}) \quad (3)$$

$$M1 = \frac{NPHI_{fl} - NPHI_{ma}}{RHO_{fl} - RHOB_{ma}} \quad (4)$$

2.2 Determination of Porosity (\emptyset)

In the present work methods which used to define Porosity are:

2.2.1 Density porosity

The mechanism for this method to determine formation porosity represent at Tool emits gamma rays, Detects returning scattered gamma rays and Gamma ray absorption is proportional to rock density. Measures density tied to lithology, porosity, and fluid content. The total Porosity was evaluated using the relationship from the density log

$$\emptyset_D = \frac{\rho_{ma} - \rho_{log}}{\rho_{ma} - \rho_{fluid}} \quad (5)$$

2.2.2 Neutron logs:

Neutron logs are porosity logs that measure the hydrogen ion concentration in a formation. Where the pores are filled with oil or water in clean formations the neutron log measures liquid-filled porosity. Porosity can be determined from a Neutron-Density log by formula

$$\emptyset = \sqrt{\frac{\emptyset_N^2 + \emptyset_D^2}{2}} \quad (6)$$

2.2.3 Effective porosity from Neutron-Density log

Effective porosity depends on the volume of shale and total porosity from this equation the effective porosity can be evaluated.

$$\phi_e = \phi_T (1 - V_{SH}) \quad (7)$$

2.3 Water saturation (Sw)

The amount of water that occupies pore space represents the saturation of water at formation. There are two methods used for determine the water saturation at these work. Archie and Indonesia methods. Archie (1942) suggested the relationship of water saturation, formation factor, resistivity of the rock, and resistivity of the water in the formation given in

$$\text{Equation } S_W = n \sqrt[n]{\frac{R_W}{\phi^m \cdot R_T}} \quad (8)$$

Indonesia equation by Poupon and Leveaux, 1971 is used to determine the water saturation. The Indonesia equation may work well and the parameter R_{sh} (resistivity of shale) is usually taken from the resistivity reading of nearby pure shale.

Indonesia equation

$$S_{Windo} = \left\{ \frac{\sqrt{\frac{1}{R_t}}}{\left(\frac{V_{sh}(1-0.5V_{sh})}{\sqrt{R_{sh}}} \right) + \sqrt{\frac{\phi_e^m}{a \cdot R_w}}} \right\}^{(2/n)} \quad (9)$$

2.3 Hydrocarbon Saturation

From effective porosity

$$\text{Hydrocarbon saturation} = (1 - \text{water saturation})$$

2.5 Netpay Thickness

Netpay Thickness calculated from log take average from pay net flag.

3. Results and Discussion

From wire line logging data

3.1. Petrophysical evaluation

3.1.1 Porosity (ϕ)

The results of total and effective porosity for each well (RB-A1, RB-B1, RB-B11 and RB-C1) from Neutron log and Neutron – Density log are listed in (Table 1).

3.1.1.1 Total porosity

The more appropriate method in this study is the combination between the neutron and density porosity logs, correlation panel showing porosity using neutron-density log (Figure 3), Iso-porosity map for Nubia A (Figure 7) and porosity results show minimum porosity value is about 13.5% represent at RB-C1 well and maximum porosity values is about 15% represent at RB-B1 well. The zone of new development for Nubia A is tending towards central part, where this zone has excellent probability for porosity and storage capacity of reservoir.

3.1.1.2 Effective porosity

From correlation panel showing effective porosity using neutron-density log (Figure 4) Effective porosity map for Nubia A (Figure 8) and effective porosity results show minimum value is about 13.2% around RB-C1 well and maximum value is about 15% around RB-B1 well. The zone of new development for Nubia A is tending towards central part, where this zone has excellent probability for effective porosity and storage capacity of reservoir.

3.1.2 Volume of shale (V_{sh})

The volume of shale is calculated from merged between two methods Gamma Ray method and Neutron Density method which gives accurate results shown in (Table 2) so that the volume of shale map can be created. Correlation panel showing volume of shale using GR log (Figure 5). Volumes of shale map for Nubian A (Figure 9) and results show that the minimum value is approximately 0.3% and the maximum value approximately 2.1%. The zone of new development for Nubia A in the studied field towards the east direction, where show a decrease in shale volume.

3.1.3 Water saturation (Sw)

Two methods have been used to calculate water saturation in different wells to choose the appropriate method. Archie method and Indonesia method (effective water saturation) the water saturation results are shown in (Table 3). From water saturation results of this study, it can be depended on water saturation calculated by Indonesia equation (S_{Windo}), where it gives accurate results with shaly formation, Panel showing the water saturation using Indonesia and Archie models (Figure 6) the iso-effective water saturation map was created for each zone.

Water Saturation variation map for **Nubia A**. The water saturation (S_w) distribution (**Figure 10**) ranges from 15.4% to 52.1%. The zone of new development for **Nubia A** in the studied field trends southeast- northwest, where show a decrease in water saturation.

3.1.4 Hydrocarbon Saturation

The following (**Table 4**) showing the effective water saturation and hydrocarbon saturation for each zone, ISO-Hydrocarbon saturation map for **Nubia A**. The Hydrocarbon saturation distribution (**Figure 11**) ranges from 47.9% to 84.6%.The zone of new development for **Nubia A** in the studied field trends northwest- southeast, where this zone has excellent probability for a reservoir.

3.1.5 Netpay Thickness

Net-Pay Thickness (**Table 4**) can be determined and calculated from different wells for each zone for Nubia Formation. From these results, Netpay thickness map can be created for each zone for Nubia Formation.

Netpay thickness map for **Nubia A** (**Figure 12**) show that the minimum thickness value is 21 ft. the maximum thickness is 137.25ft.The zone of new development for **NubiaA** in the studied field trends southwest-northeast, where this zone has excellent probability for a reservoir

3.2 Lithological Identification Techniques

The crossplots combinations are discussed in **Poupon et al. (1970)**; **Schlumberger (1974)**; **Dresser (1979)**.The lithology from logs can be deduced by using the composite log and the crossplots. The crossplot used in this study is the Neutron – Density crossplot. In the present study, the Neutron – Density crossplots have been applied on the Zone **Nubia A** at Nubia Formation in the studied wells.

In RB-A1 well, the major of the plotted points (**Figure 13**) are shifted toward sandstone line with average porosity ranging from 6% to13%. Some other points are scattered between limestone and dolomite lines due to shale effect or borehole conditions. This indicates the presence of mixed lithology (sandstone, shale and limestone).

In RB-B1 well, the major of the plotted points (**Figure 14**) are toward sandstone line with average porosity ranging from 5% to 14%. Some other points are scattered between limestone and sandstone lines. This indicates the presence of mixed lithology (sandstone and limestone).

In RB-B11 well, the major of the plotted points (**Figure 15**) are between limestone and sandstone lines with average porosity ranging from 8% to 16%. Some other points are scattered between limestone and dolomite lines. This indicates the presence of mixed lithology (sandstone, limestone and dolomite).

In RB-C1 well, the major of the plotted points (**Figure 16**) are shifted toward sandstone line with average porosity ranging from 5% to 14%. Some other points are scattered between limestone and sandstone lines. This indicates the presence of mixed lithology (sandstone, shale and limestone).

3.3 Cut-off determination

3.3.1 Cut-off of shale content

To identification of total sand intervals and to tell sand from shale, Shale content cut-off have been used which can be determined according to shale content-effective porosity relationship of a number of wells and Gamma ray log (**Darling, 2005**; **Ghanima et al., 2020**).**Figure 17** shows the shale content-porosity crossplot and Gamma ray log used for determination of shale content cut-off. The plot shows the volume of shale cut-off (V_{sh}) value for reservoir and non-reservoir rock determined is 0.5, meaning that rocks with equal to or less than 50 percent of shale are regarded as reservoirs, while rocks with more than 50 percent of shale are regarded as non- reservoir rock.

3.3.2 Water saturation cut-off

To discriminate between netpay and non-pay intervals in the porous interval water saturation cut-off have been used, determined according to effective water saturation-effective porosity crossplot and gamma ray log. **Figure 18** shows an example. Intervals that have water saturation greater than 50 percent are assumed to be non-productive intervals, while intervals with water saturation of less than 50% are pay zones.

3.3.3 Porosity cut-off

The porosity cut-off is used to perceive between porous & permeable and tight sand intervals in the gross sand interval, equivalent to the porosity conforming to the minimum permeability allows oil and gas flow (**Darling 2005**; **El-Din et al., 2013**).It can be seen porosity of 10% can be taken as the cut-off points for reservoir and non-reservoir.

4. Conclusions

Nubia Formation is very good reservoir rock in most intervals, where the interpretation of the well logging data indicates that the total porosity range from 13.8% to 15%, effective porosity range from 13.2% to 15%, shale content ranges between 0.3% to about 2.1%, water saturation from 15.4% to about 52.1%, hydrocarbon saturation range from 47.9% to 84.6% and Netpay thickness ranges between 21 ft. to about 137.25ft. From Lithological Identification Techniques for Nubia A indicates the presence of mixed lithology sandstone, shale, dolomite and limestone. The development in Ras Budran field for NubiaA is towards central part and northwest- southeast for Nubia3 was shown by the increasing of effective porosity and hydrocarbon saturation respectively. There is a good opportunity to drill other Exploratory and development wells to enhance the productivity of the study area because the study area is containing valuable amount of hydrocarbon accumulation.

New contour maps at reservoir levels had been constructed. The new set of maps will be used as the basis for building a new static and dynamic model for Ras Budran Field in addition to considering them as the common basis for future wells' planning.

5. Acknowledgements

Ahmed Galal would like to thank the Egyptian General Petroleum Corporation (EGPC) and Suez oil company (SUOCO) for supplying the well log data for this study.

Nomenclature

GR: Gamma ray

$S_{W\text{ Archie}}$ is Water saturation

V_{sh} : Volume of shale using Archie model for saturation

\emptyset : Porosity

\emptyset_D : Density porosity

\emptyset_e : Effective Porosity

\emptyset_T : Total Porosity

S_W : Water saturation

M: formation factor

N: formation factor

R_W : Resistivity of water

R_T : Resistivity of rock

\emptyset_{ND} : Neutron density porosity

\emptyset_N is Neutron porosity

V_{shGR} : Volume of shale using gamma ray method

V_{shND} : Volume of shale using Neutron-Density method

$V_{shFinal}$: Final Volume of shale

$S_{W\text{ indo}}$ is Water saturation using Indonesia model for saturation

Table1: Total and effective porosity by using Neutron and Neutron-Density methods.

Well Name	Zone	\emptyset_N	\emptyset_{ND}	\emptyset_e
RB-A1	Nubia A	0.0887	0.138	0.137
RB-B1	Nubia A	0.10	0.15	0.15
RB-B11	Nubia A	0.119	0.144	0.142
RB-C1	Nubia A	0.086	0.135	0.132

Where; \emptyset_N is Neutron porosity..., \emptyset_{ND} Neutron-Density method for porosity and \emptyset_e is effective porosity.

Table2. The actual parameters used to evaluate volume of shale (V_{sh}) by using gamma ray and neutron density methods

Well Name	Zone	V_{shGR}	V_{shND}	$V_{shFinal}$
RB-A1	Nubia A	0.150	0.005	0.005
RB-B1	Nubia A	0.093	0.006	0.003
RB-B11	Nubia A	0.0711	0.035	0.021
RB-C1	Nubia A	0.203	0.009	0.009

Where;

V_{shGR} is volume of shale using gamma ray method...

V_{shND} is volume of shale using Neutron-Density method... and

$V_{shFinal}$ is volume of shale by merged method using gamma ray and Neutron-Density methods

Table 3 .Water saturation by using Archie and Indonesia models for saturation

Well Name	Zone	$S_{W Archie}$	$S_{W indo}$
RB-A1	Nubia A	0.237	0.238
RB-B1	Nubia A	0.162	0.163
RB-B11	Nubia A	0.521	0.521
RB-C1	Nubia A	0.143	0.154

Where; $S_{W Archie}$ is Water saturation using Archie model for saturation and $S_{W indo}$ is Water saturation using Indonesia model for saturation

Table 4 Water and Hydrocarbon saturation and Net pay thickness of four wells.

Well Name	Zone	water saturation	Hydrocarbon saturation	Net pay thickness (ft)
RB-A1	Nubia A	0.238	0.762	137.25
RB-B1	Nubia A	0.163	0.837	54.6
RB-B11	Nubia A	0.521	0.479	21
RB-C1	Nubia A	0.154	0.846	53.4

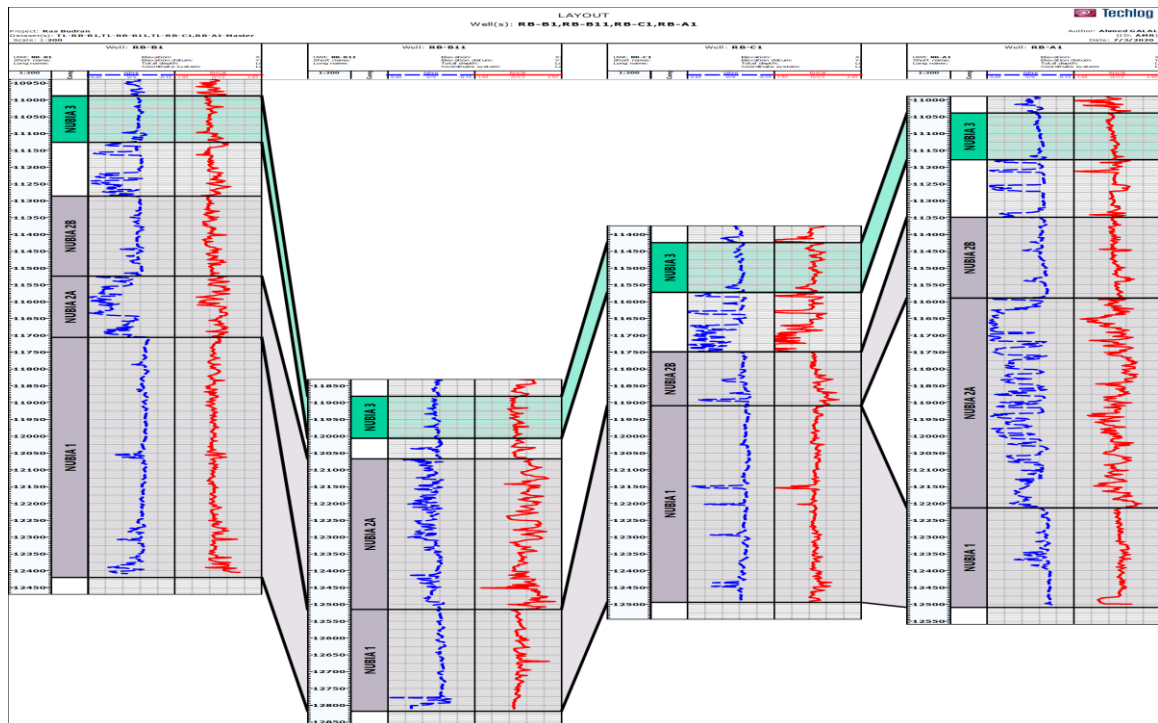


Figure 3 correlation panel showing porosity using neutron-density log

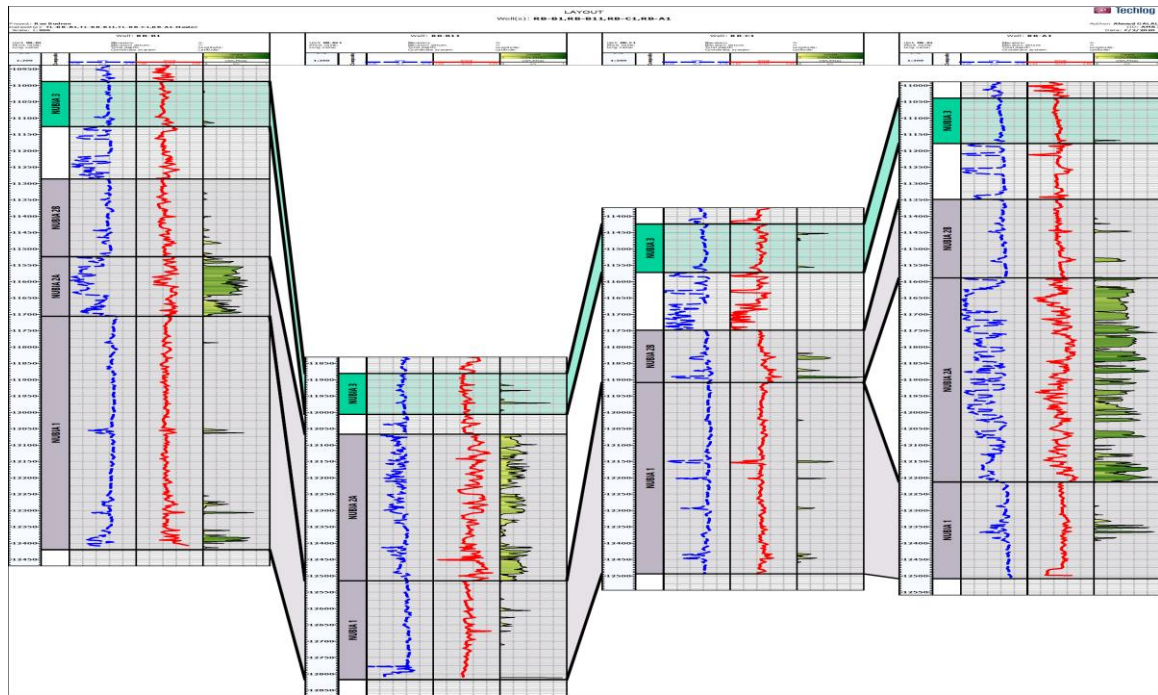


Figure 4 correlation panel showing effective porosity using neutron-density log

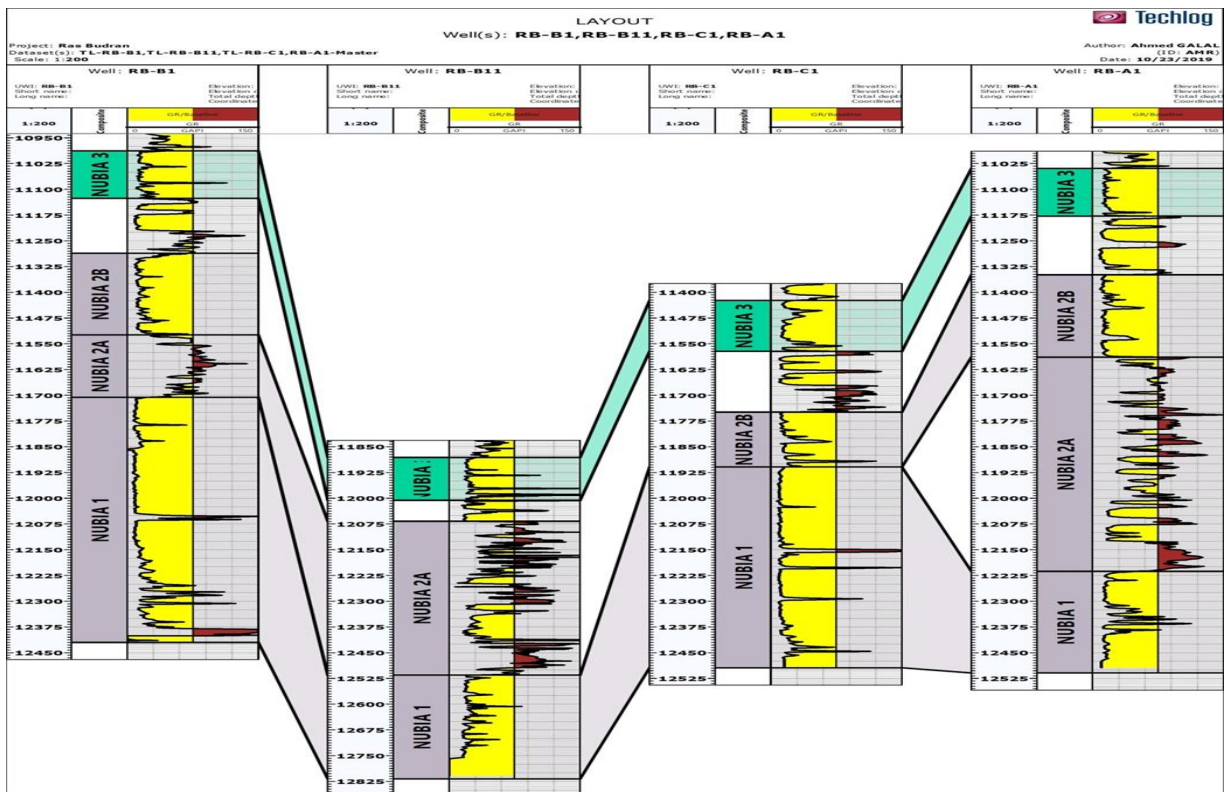


Figure 5 Correlation panel showing volume of shale using GR log,

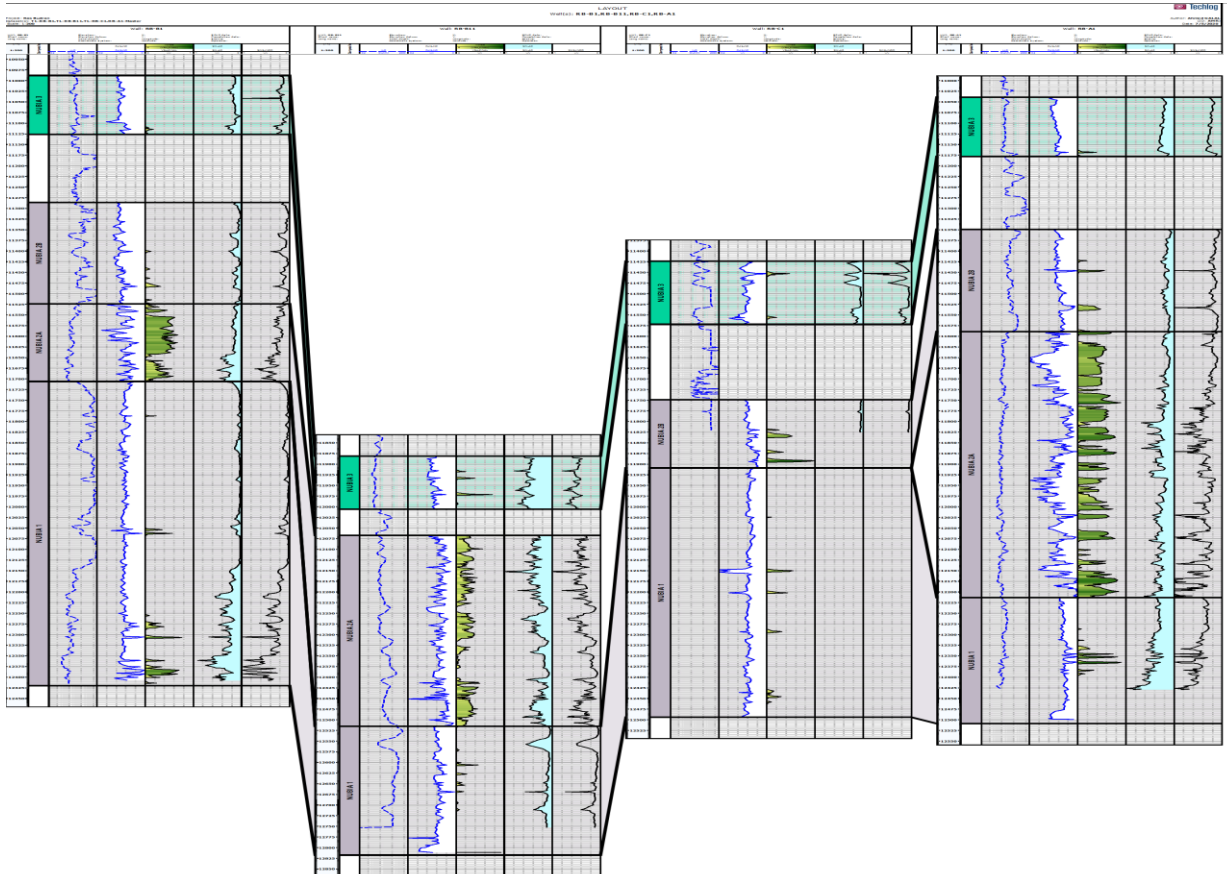


Figure 6 Panel showing the water saturation using Indonesia and Archie models

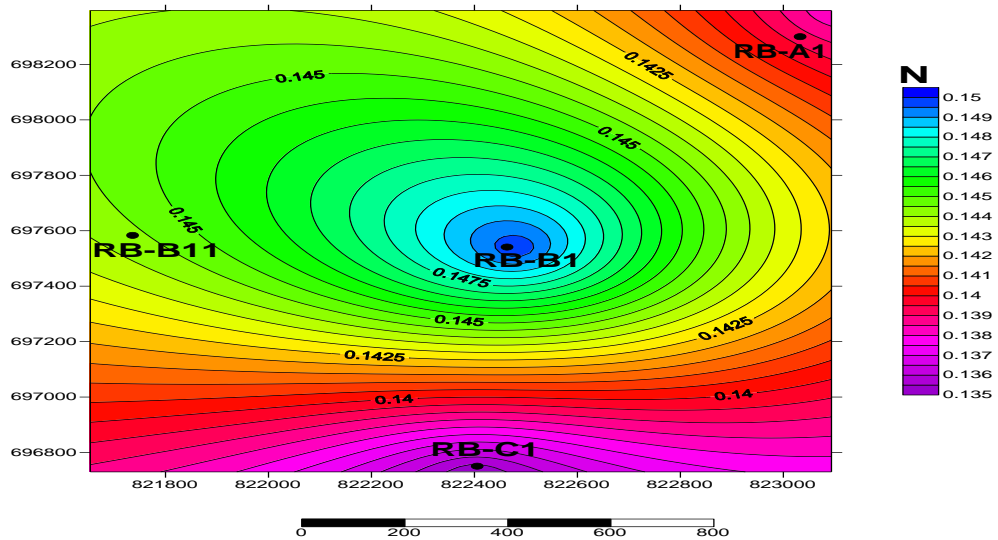


Figure 7 Iso-porosity map for Nubia A

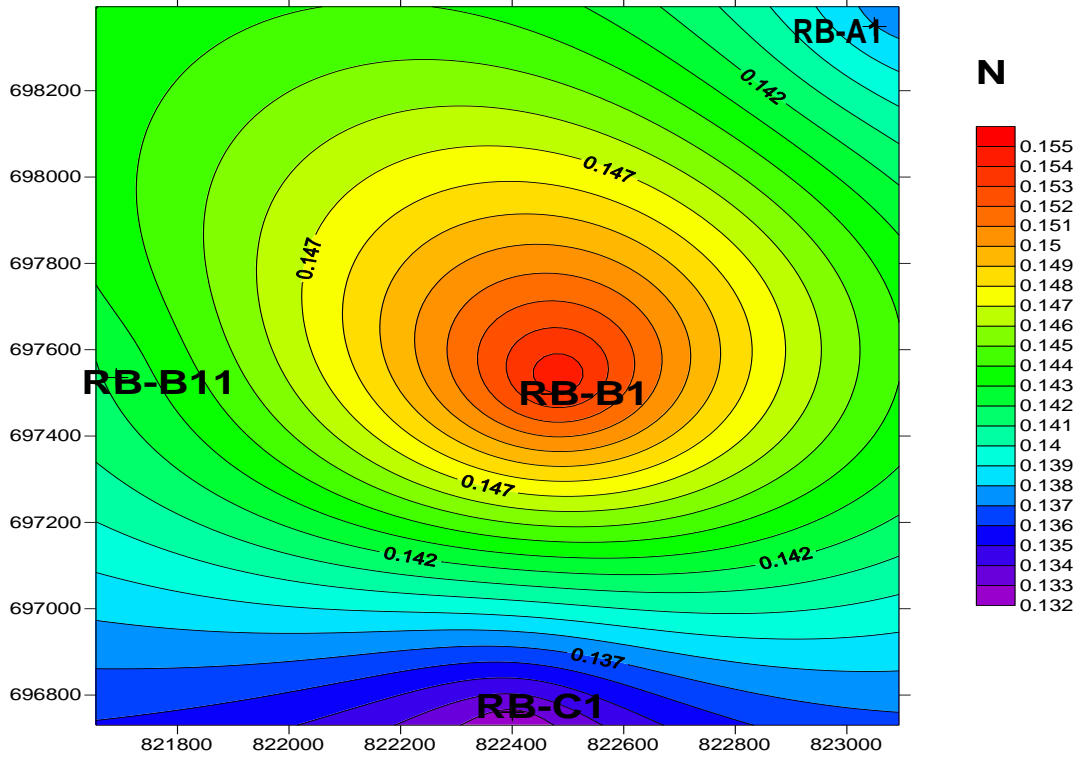


Figure 8 Effective porosity map for Nubia A

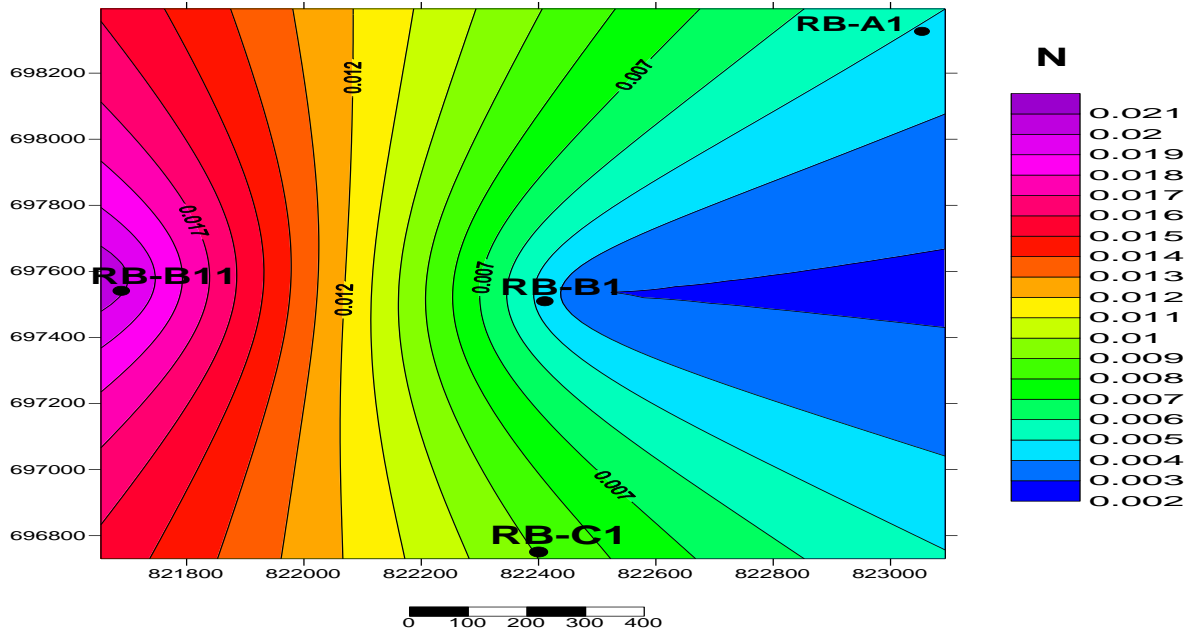


Figure 9 Volume of shale map for Nubia A

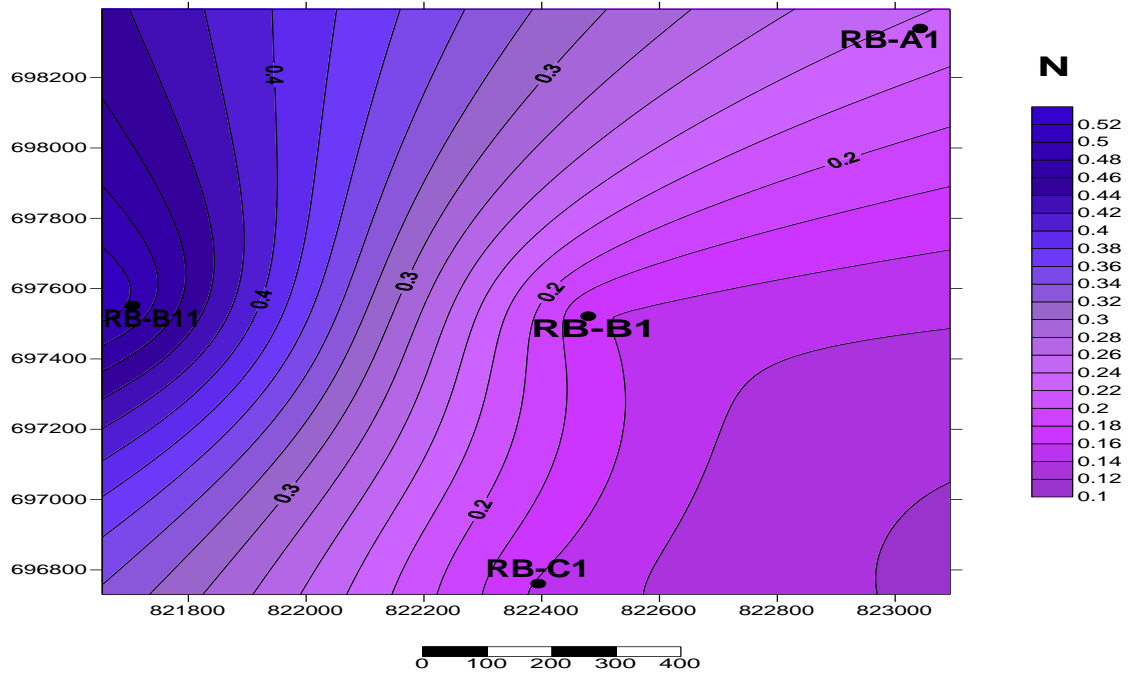


Figure 10 Water Saturation map for Nubia A

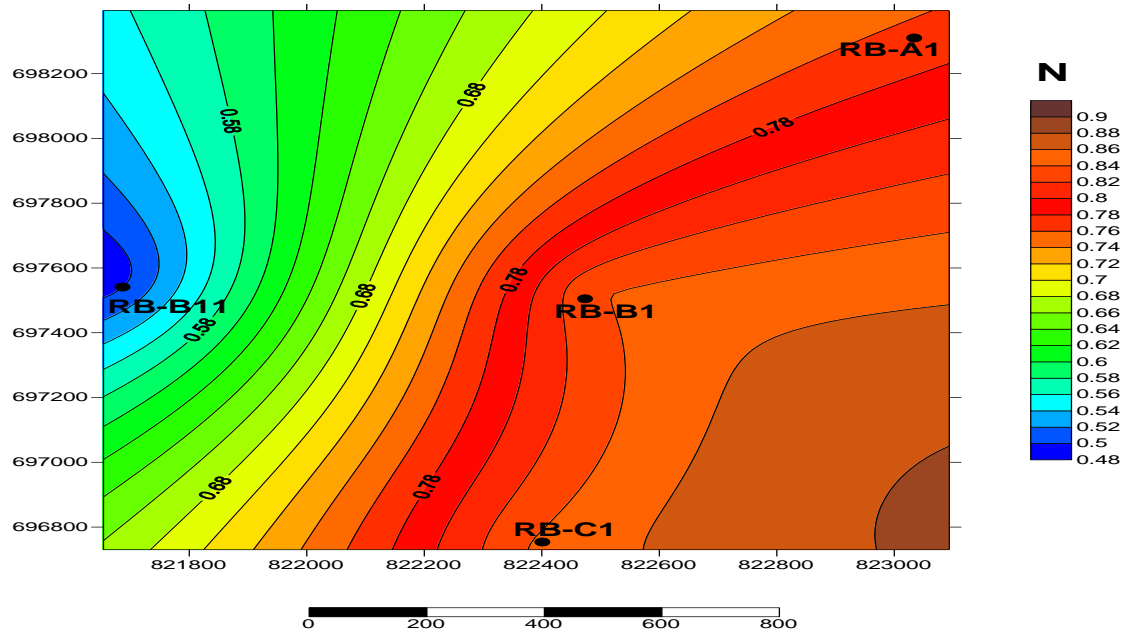


Figure 11 Hydrocarbon saturation map for Nubia A

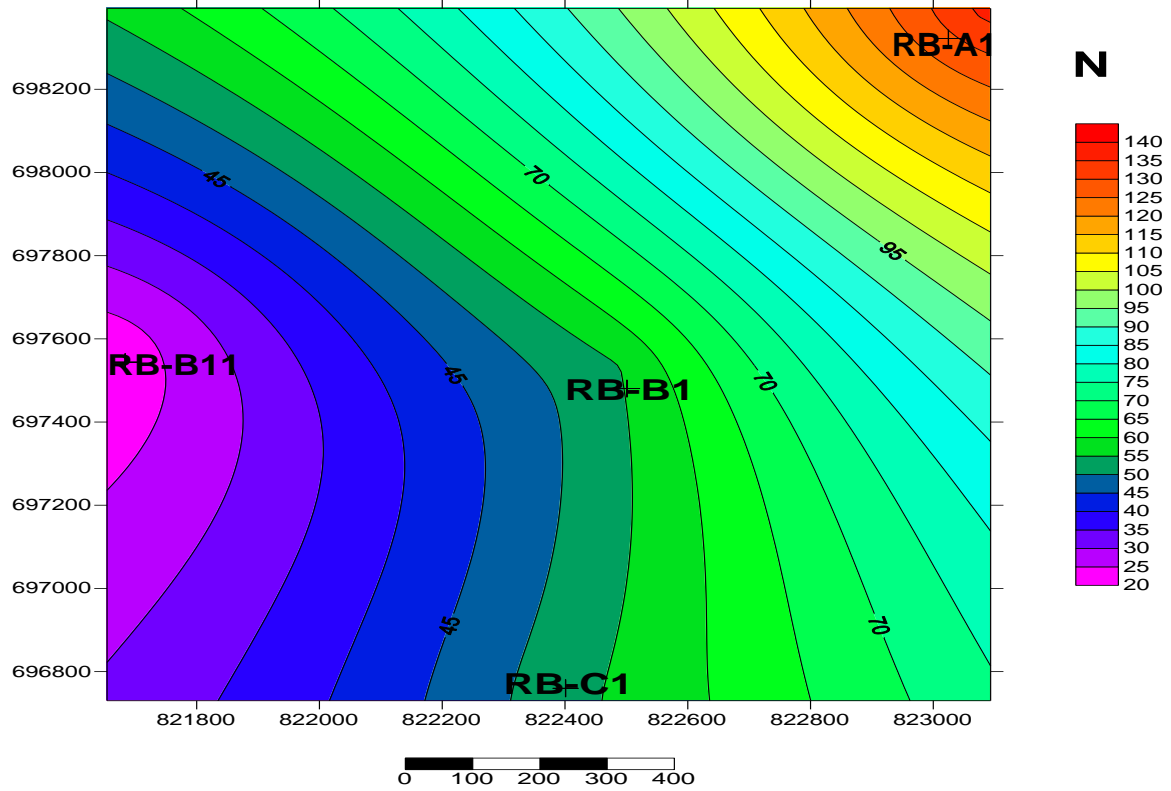


Figure 12 Netpay thickness map for Nubia A

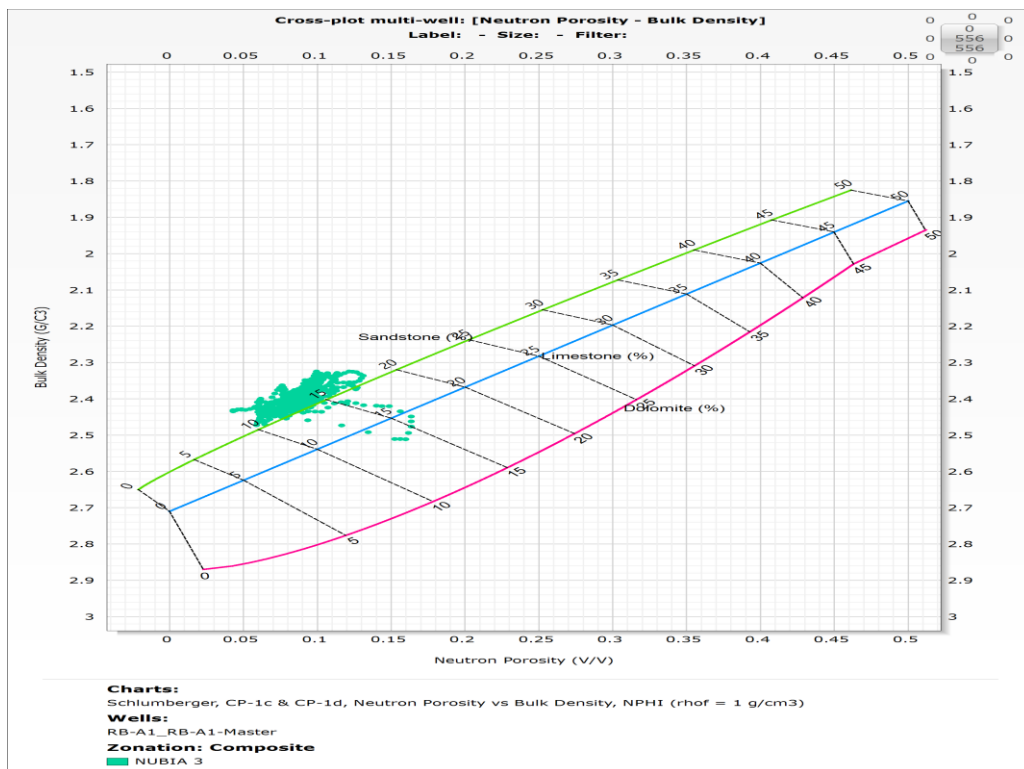


Figure 13 Neutron- Density crossplot for RB-A1 well.

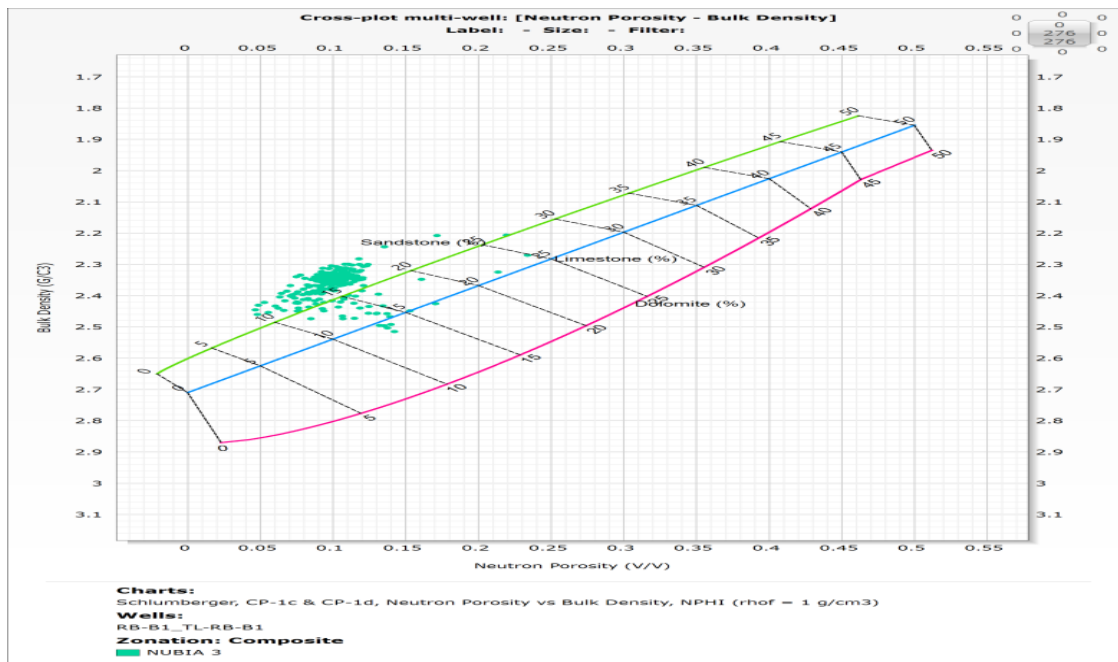


Figure 14 Neutron- Density crossplot for RB-B1 well.

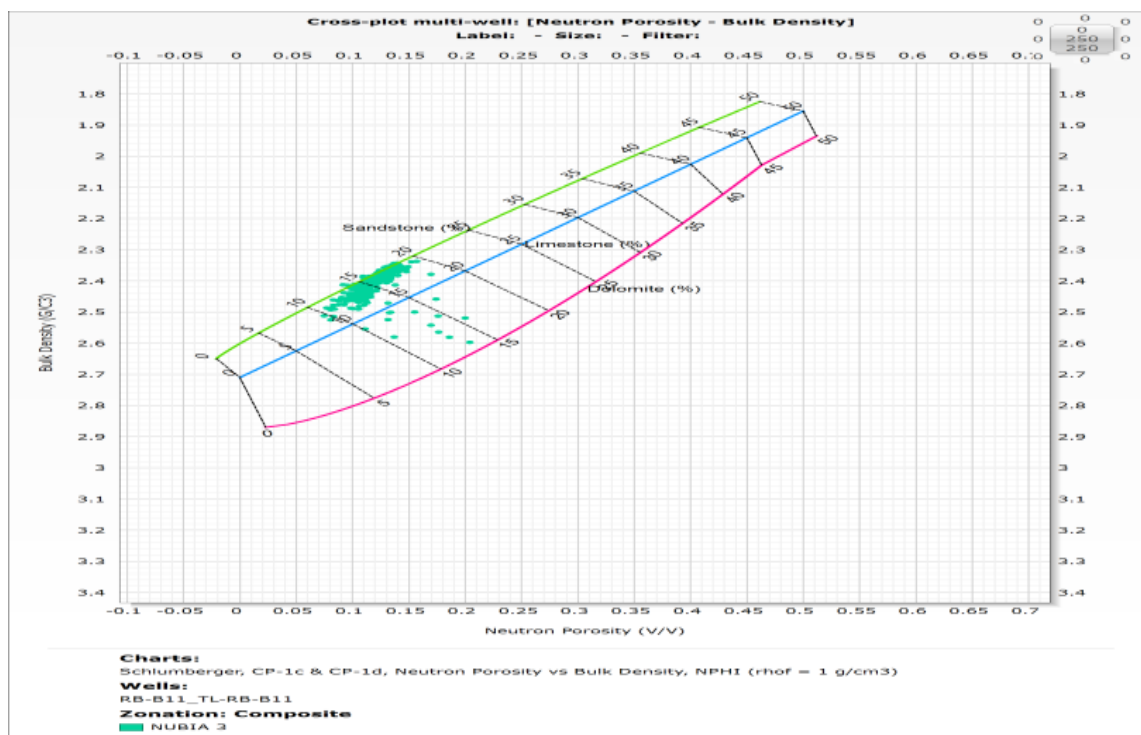


Figure 15 Neutron- Density crossplot for RB-B11 well.

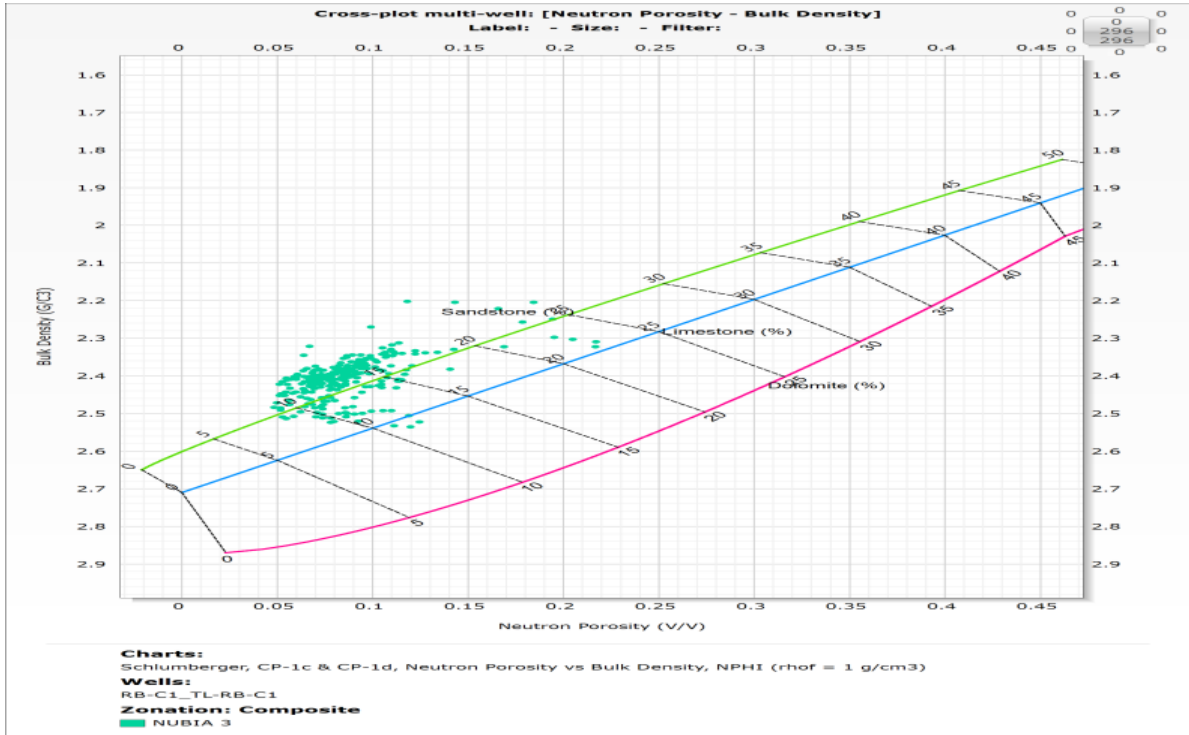


Figure 16 Neutron- Density crossplot for RB-C1 well.

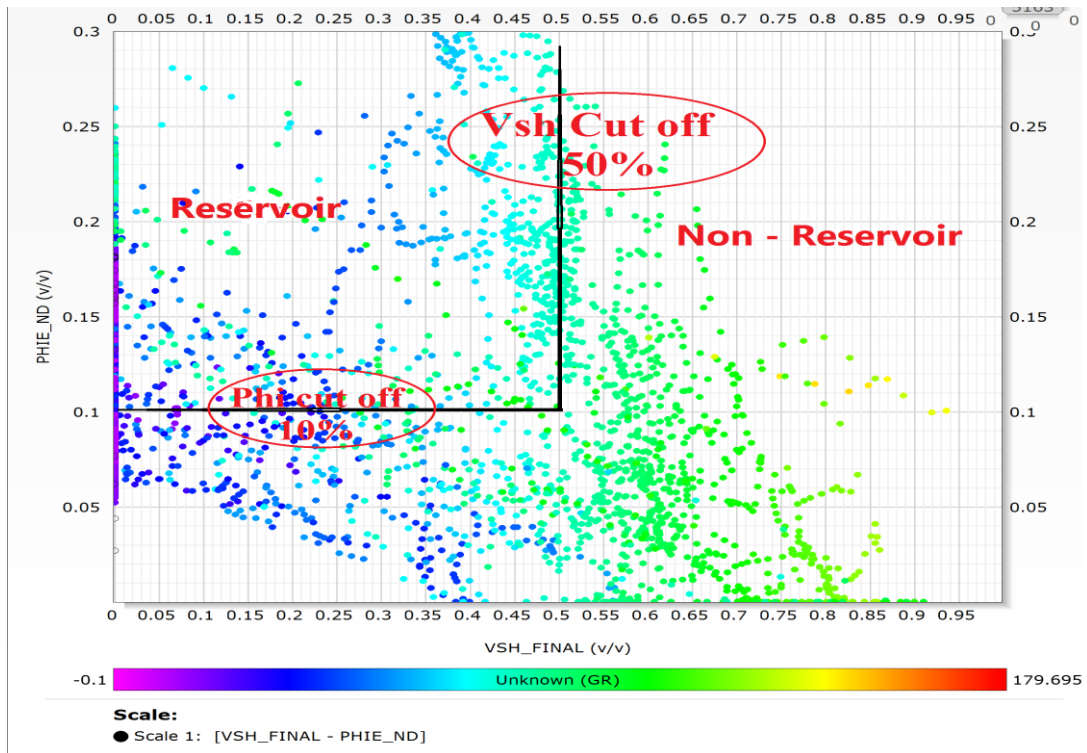


Figure 17 Shale content versus porosity crossplot and gamma ray log for cut-off determination

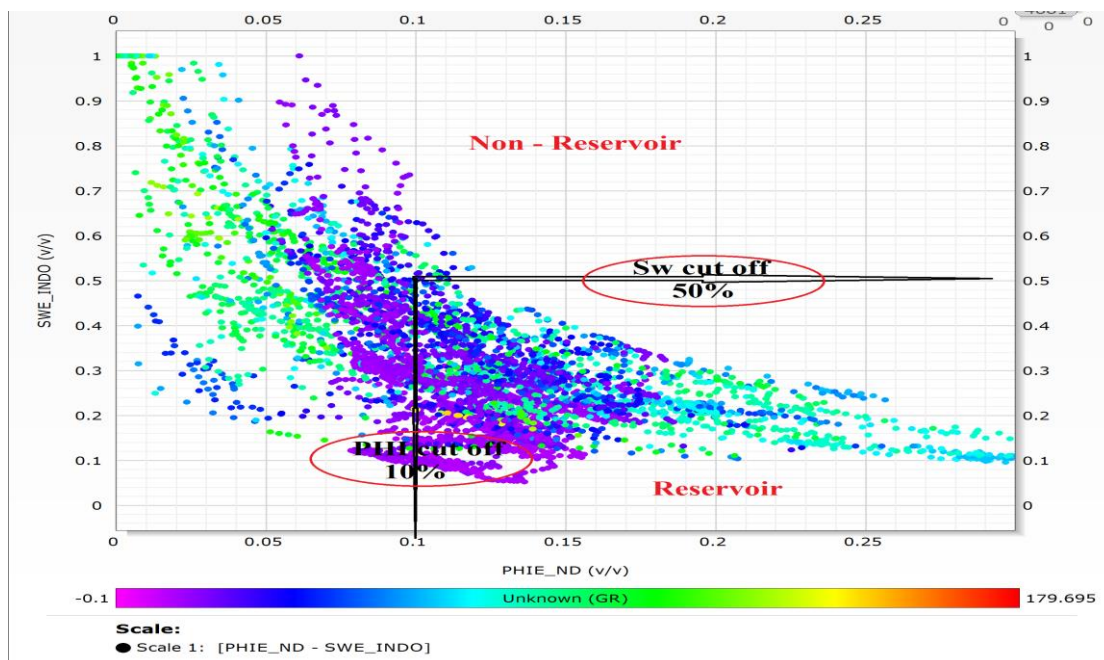


Figure 18 Porosity-water saturation crossplot for cut-off determination

References

1. Abd El Gawad, M. (1970). The Gulf of Suez; A brief review of stratigraphy and structure. 'Review Phil., Trans. Roy. Soc. Lond, A., v. 267, 41-48.
2. Alsharhan, A. S., and Salah, M. G. (1995). Geology and hydrocarbon habitat in rift setting: northern and central Gulf of Suez, Egypt. Bulletin of Canadian Petroleum Geology, 43(2), 156-176.
3. Alsharhan, A.S. (2003). Petroleum geology and potential hydrocarbon plays in the Gulf of Suez rift basin, Egypt. 'Review American Association of Petroleum Geologists Bulletin, 87(1), 143-180.
4. Archie, G. E., (1942): Electrical resistivity log as an aid in determining some reservoir characteristics, Trans., AIME, 146, 54-61.
5. Azab, A.A. Ramadan, M.A. Elsayy, M.Z. (2019) An integrated analysis of gravity and well data for deep-seated structural interpretation: a case study, from RasBudran oil field, Gulf of Suez, Egypt". Journal of Petroleum Exploration and Production Technology 9:177-189)
6. Beleity, A.M., Ghoneim, M., Hinawi, M., Fathi, M., Gebali, G., and Kamal, M. (1986). In Paleozoic stratigraphy, paleogeography and paleotectonics in the Gulf of Suez (pp. 21). Paper presented at the 8th Exploration seminar, Egyptian General Petroleum Cooperation, Cairo.
7. Bobbitt, J.E., and Gallagher, D.J. (1978). In The Petroleum Geology of the Gulf of Suez (pp. 375-380). Paper presented at the 10th annual OTC Houston.
8. Dresser Atlas. (1979). Log Interpretation Charts. Houston (Texas): Dresser Industries Inc.; p. 107.
9. Darling, T. (2005), Well Logging and Formation Evaluation, Elsevier Inc., pp. 1-326
10. El Nady, M.M., Ramadan, F.S., Hammad, M.M., Lotfy, N.M., (2015). Evaluation of organic matters, hydrocarbon potential and thermal maturity of source rocks based on geochemical and statistical methods: case study of source rocks in RasGharib oilfield, central Gulf of Suez, Egypt. Egyptian Journal of Petroleum 24 (2), 203-211.
11. Elnaggar, A.A., Kassab, M.A. and Abass, A.E. (2018). Reservoir characterization utilizing core and wire line logging data for Kareem sandstone, Ashrafi oil Field, Gulf of Suez, Egypt, Egypt. J. Petrol. 27, 1013-1027.
12. El sayy, M, Z: (2016): Study of Petroleum System in Ras Ghara Oil Field, Gulf of Suez, Egypt. Ph.D. Thesis, ZagazigUniversty, PP. 1-242.
13. Ghanima, A., Kassab, M.A. and Abass, A.E. (2020). Petrophysical evaluation of clastic Upper Safa Member using well logging and core data

- in the Obaiyed field in the Western Desert of Egypt. Paper presented at Egyptian Journal of Petroleum.
14. Ghorab, M.A. (1961). In Abnormal Stratigraphic features in RasGharib Oilfield (Vol. 2, pp. 1-10). Paper presented at the 3rd. Arab Petroleum Cong., Alexandria.
 15. Moustafa, A.M., 1976. Block faulting in the Gulf of Suez. In: Proceedings of the 5th Egyptian General Petroleum Corporation Exploration Seminar, Cairo, Egypt, and vol. 35.
 16. Patton, T.L., Moustafa, A.R., Nelson, R.A., Abdine, S.A., (1994). Tectonic evolution and structural setting of the Suez rift. In: Landon, S.M. (Ed.), Interior Rift Basins, vol. 59. AAPG Memoir, pp. 9–55.
 17. Poupon A, Leveaux J (1971). Evaluation of Water Saturation in Shaly Formations, the SPWLA 12th Annual Logging Symposium, Dallas, Texas, 2-5 May. SPWLA-1971-O.
 18. Russegger, J.R. (1937). Kreide und sandsteiniEinflussvon Granit auf Letzern. 'Review N. Jb. Mineral, 1837, 665-669.
 19. Said, R. (1962). Geology of Egypt. 377 pp. Amsterdam, Elsevier Science Publishing Company Inc.
 20. Schlumberger, (1995). Well Evaluation Conference. pp. 87 Egypt. Paris, France.
 21. Schlumberger. (1974). Log interpretation manual. Vol. II (Application). New York: Schlumberger Limited; p. 116 p.
 22. Schlumberger. (1984). In Geology of Egypt (pp. 1-64). Paper presented at the Well Evaluation Conference, Schlumberger, Cairo.
 23. Steen, G. (1982). Radiometric age dating and tectonic significance of some of Gulf of Suez igneous rocks. In Hunter, G. (Ed.), 6th Exploration Seminar (20), Egyptian General Petroleum Cooperation, Cairo.
 24. El-Din, E.S., Mesbah, M.A., Kassab, M.A., Ibtehal, F.M., Cheadle, B.A., and Teama, M.A. (2013). Assessment of petrophysical parameters of clastics using well logs: The Upper Miocene in El-Wastani gas field, onshore Nile Delta, Egypt. *Petrol. Explor. Develop*, 2013, 40(4): 488–494.
 25. Zahran, M.E., and Meshref, W.M. (1988). In The northern Gulf of Suez: Basin evolution, stratigraphy and facies relationships (pp. 110-125). Paper presented at the 9th Exploration and Production Conference, Egyptian General Petroleum Corporation, Cairo.
 26. Zein El-Din, M.Y., Abd El-Gawad, A.E., and Doniya, M.G. (1997, 22-26th September 1997). In Evaluation of Source Rocks in the South Ghara Area, Gulf of Suez, Egypt. Paper presented at the 18th International Meeting on organic Geochemistry, Netherlands. 22-26th September 1997.